Full Description of Methods

Subjects

Dlg4$^{-/-}$ were generated as recently described (1, 2). For the current study, the *Dlg4* null mutation was repeatedly backcrossed into the C57BL/6J strain. Analysis of 150 SNP markers at ~15-20 megabase intervals across all autosomal chromosomes confirmed 95% C57BL/6J congenicty (JRS Allele Typing Services, The Jackson Laboratory, Bar Harbor, ME). To avoid potential phenotypic abnormalities resulting from genotypic differences in maternal behavior and early life environment (3), *Dlg4*$^{+/+}$ and *Dlg4*$^{-/-}$ were littermates generated from *Dlg*$^{+/-}$ x *Dlg4*$^{+/-}$ matings. We found that homozygous deletion of *Dlg4* adversely affected survival to weaning age (Mendelian ratio 1.5: 2.0: 0.5), as previously found in another line of *Dlg4* null mutants (4), for reasons that remain undetermined.

Mice were bred and maintained at The Jackson Laboratory (Bar Harbor, ME) and shipped to the NIH at 7-9 weeks of age. Mice were housed with same-sex littermates in a temperature and humidity controlled vivarium under a 12 h light/dark cycle (lights on 0600 h). Testing began after at least 1 week of acclimation to the animal facility. Males and females were used except in social tests. Sex was included as a variable in statistical models but found not to influence genotype differences on any task and therefore collapsed across groups to increase the power of the statistical analysis. To minimize potential carry-over effects (5), multiple cohorts were tested, with a limited number of tests conducted in any given cohort and putatively more stressful tests conducted later in the sequence.

For all experiments, mice were first acclimated to the test room for 1 hr. The experimenter remained blind to genotype during testing (subjects were identified by subcutaneously implanted microchips or ear notch). The number of mice tested is given in the Fig legends. All experimental procedures were approved by the National Institute on Alcohol Abuse and Alcoholism Animal Care and Use Committee and strictly followed the NIH guidelines 'Using Animals in Intramural Research.'

Health, neurological and sensory assessment

Basic screen

Mice were evaluated for physical health, sensory and neurological functions, and empty cage behaviors, as described previously (6, 7). Basic physical health was evaluated by examining for missing whiskers, bald patches, exophthalmus, straub tail, kinked tail, kyphosis, lordosis, body weight, and core body temperature. Simple sensory reflexes were measured via orienting responses to an approaching hand and to physical touch, and via palpebral closure on touch of the eye, twitch of the pinna on touch and an orienting response to tail pinch. Basic motor and neurological function was assessed by observing for splayed limbs, forepaw clutch and hind limb clutch when mice were suspended upside down by the tail. The mouse was placed in a bare empty home cage and observed for the presence of freezing, trembling, wild running, grooming, sniffing, licking, rearing, jumping, spontaneous seizure, defecation, urination, head bobbing, circling, abnormal gait, and retropulsion over 60 sec. Genotypes were compared using Mann-Whitney non-parametric tests. The threshold for statistical significance for this and all other statistical analyses was $p<.05$.

Startle and sensorimotor gating

Acoustic startle and prepulse inhibition of the startle response, a measure of sensorimotor gating, was measured as previously described (8, 9). The mouse was placed into a clear Plexiglas cylinder in 1 of 4 SR-Lab System startle chambers (San Diego Instruments, San Diego, CA) for a 5 min acclimation period. A 65 dB broadband background noise was presented during acclimation and throughout the test session. During the test session, mice were presented with startle trials (40-msec 120-dB broadband sound pulse) and prepulse+startle trials (20-msec noise prepulse sound followed, 100 msec later, by a 40-msec 120-dB broadband sound pulse). The prepulse+startle trials were preceded and followed by 5 pulse alone trials, which were not included in the analyses. Test trials consisted of 10 trials of 3 different intensities (3, 6, and 12 dB above background). Each trial type was presented 10 times with a variable interval of 12-30 sec between each presentation. Basal activity in the startle chambers was measured during no-stimulus trials. Startle amplitude was measured every 1 msec, over a 65 msec period beginning at the onset of the startle stimulus. The peak startle amplitude over the sampling period was taken as the dependent variable. Whole-body startle responses were measured via vibrations transduced into analog signals by a piezoelectric unit attached to the platform on which the cylinders rested. Prepulse inhibition of startle was calculated as 100-[(startle response for prepulse+startle trials/startle response for startle-alone trials)x100]. Genotypes were compared for baseline movement and startle amplitude using unpaired *t*-tests. Genotype x prepulse intensity effects on prepulse inhibition were analyzed using 2-factor analysis of variance (ANOVA), with repeated measures for intensity.

Hot plate nociception

Sensitivity to painful stimuli was assessed via the hot plate test. The apparatus was a flat plate (Columbus Instruments, Columbus, OH) heated to 55ºC on which the mouse was placed (7). The latency to show a hind paw shake or lick was timed by an observer, with a maximum response latency of 30 sec. Genotypes were compared using unpaired *t*-tests.

Olfactory processing of non-social and social scents

Olfactory processing of both non-social and social scents was assessed using a habituation-dishabituation test based on methods previously described (10). Mice were first habituated to a cotton-tip applicator by inserting the applicator with the tip soaked with tap water into the home cage 3 times for 180 sec at a time. Next, mice were exposed to the applicator with the tip soaked in banana scent [~0.25 mL food flavoring (McCormick & Co, Inc, Hunt Valley, MD) diluted 1:100 with tap water], then almond scent [~0.25 mL food flavoring (McCormick & Co, Inc, Hunt Valley, MD) diluted 1:100 with tap water], and finally male urine [~0.25 mL collected from ~7 male C57BL/6J mice, diluted 1:1]. Each scent was presented 3 times in succession for 180 sec at a time. The time spent sniffing (nose within 2 cm) the applicator tip was recorded using Hindsight scoring software. Genotype x scent-presentation effects were analyzed using 2-factor ANOVA, with repeated measures for scent-presentation, followed by Fisher's LSD *post hoc* tests to compare genotypes and paired *t*-tests to compare scent-presentations within genotype.

Repetitive behaviors

T-maze spontaneous alternation

The discrete trial T-maze spontaneous alternation task was conducted as previously described (11, 12). The apparatus was an enclosed T-shaped maze constructed of black Plexiglas. The start arm was 8.5 x 10.5 x 33.0 cm and the 2 choice arms were each 8.5 x 10.5 x 30.0 cm. Black Plexiglas dividers were inserted into the start arm to create a start box and placed at the entrance of a choice arm to sequester mice in the arm after a choice was made. Each trial commenced with mice placed in the start box for 5 sec. The insert was then removed to allow mice to run the start arm and select a choice arm (choice=all four paws in an arm), in which they were confined for 30 sec (sample phase). Mice were returned to the start box for 5 sec and then allowed to make another choice (choice phase). There were 10 trials (i.e., sample+choice phases), with a 15 min inter-trial interval. Testing was conducted under normal room lighting. Spontaneous alternation was compared across genotypes and compared to chance (50%) in each genotype using *t*-tests.

Grooming in novel cage and homecage

Mice were observed for grooming based on methods modified from those previously described (13, 14). Grooming of the face, head, or body was recorded 1) for a 10 min test in a novel empty cage filled with a thin-layer of clean bedding and then 2) immediately after being returned (individually) back to the home cage. This procedure was designed to measure grooming in both anxiety-provoking and familiar contexts. Cumulative grooming in each context was compared between genotypes using unpaired *t*-test.

Marble burying in novel cage and homecage

Marble burying was tested based on methods previously described (13, 15). Twenty-five marbles (1.5 cm diameter) were evenly placed in rows of 5 in the center of a novel cage filled with clean sawdust bedding to 3 cm in depth. The mouse was transferred from the home cage to the novel cage and the number of marbles that were at least 2/3 buried in a 30-min test session recorded. The mouse was then returned (individually) back to the home cage which now contained 25 marbles (configured as in the novel cage) and the number of marbles buried in a 30-min test session recorded. This procedure was designed to measure burying in both anxiety-provoking and familiar contexts. Marbles buried was compared between genotypes using unpaired *t*-test.

Communicative and social behaviors

Ultrasonic vocalization

Male mice were tested for ultrasonic vocalizations (USVs) to a female stimulus mouse in estrous based on methods previously described (16-18). Estrous stage was determined by visual inspection of the vagina, as described (19). After single housing in a clean novel cage for 1 hr, a novel female mouse was introduced and USVs recorded for 5 min. Different females were used for each subject. USVs were recorded by Ultrasound microphone (Avisoft UltraSoundGate condenser microphone capsule CM16, Avisoft Bioacoustics, Berlin, Germany) suspended approximately 20 cm above the testing cage and Avisoft Recorder software (Version 3.2) (250 kHz sampling rate, 16 bit format).

For acoustical analysis, recordings were transferred to Avisoft SASLab Pro (Version 4.40) and a fast Fourier transformation (FFT) was conducted. Spectrograms were generated with a FFT-length of 512 points and a time window overlap of 75% (100% Frame, Hamming window). The spectrogram was produced at a frequency resolution of 488 Hz and a time resolution of 1 msec. A lower cut-off frequency

of 40 kHz was used to reduce background noise outside the relevant frequency band to 0 dB. Call detection was provided by an automatic single threshold-based algorithm and a hold-time mechanism (hold time: 0.01 sec). An experienced user checked the accuracy of call detection. Genotypes were compared for the latency to first call and total number of calls using unpaired *t*-tests.

Free dyadic social interaction

Free social interaction was measured during a didactic encounter with a novel conspecific as previously described (20). The mouse was acclimated to a clean empty cage for 60 min. An unfamiliar weight-matched male C57BL/6J stimulus mouse (same stimulus mouse not used more than once per day) was then introduced into the cage. The mouse was scored over a 10 min test session using Hindsight scoring software (Scientific Programming Services, Wokingham, UK) for direct contact of the nose with the anogenital region or non-anogenital regions of the stimulus mouse (combined=total social interaction), as well as aggressive behavior (bite attacks, wrestling). Genotypes were compared using unpaired *t*-tests.

Social approach

Social approach behaviors were tested as previously described (18, 21, 22). To allow acclimation to the environment, the mouse was first placed in a 40 x 13 x 35 cm central area of a 39 x 39 x 35 cm square arena (50 lux) constructed of white Plexiglas for 40 min. The mouse then had access to the whole arena for a 10 min test. On 1 side of the arena, there was an unfamiliar male C57BL/6J mouse inside a 10.5-diameter cage (inverted 'pencil holder'), with 1 cm-spaced bars to allow physical contact (23). On the opposite side, there was a duplicate cage that was empty. The spatial location of mouse-containing cage was counterbalanced across genotypes. Investigation of the social or empty cage was recorded using Hindsight scoring

software when the nose of the test mouse was in contact with the cage. Immediately after the 10-min social vs. empty test, a novel unfamiliar male C57BL/6J mouse was placed in the empty cage and investigation of the novel and now-familiar stimuli was measured as above. Mice showing aberrantly minimal (<5% time) or abnormally high (>4 standard deviations) investigation of any stimulus were excluded from the analysis. Genotypes were compared for the duration and frequency of investigations, and transitions across the arena from one stimulus to the other using 2-factor ANOVA, with repeated measures for stimulus, followed by Fisher's LSD *post hoc* tests.

Effects of MPEP on social approach

The social approach test was repeated (in a new cohort) as above 30 min after intraperitoneal (i.p. in a volume of 10 mL/kg body weight) injection of 10 mg/kg 2-methyl-6-phenylethynyl-pyridine (MPEP) or saline vehicle. This dose was selected based on previous studies examining effects of MPEP on behaviors in mouse mutant models of neurodevelopmental disorders (14, 24). Genotype x stimulus x drug effects were analyzed using 3-way ANOVA followed by Fisher's LSD *post hoc* tests.

Object approach

As a non-social control test, the social approach test was repeated (in a different cohort) as above with the social stimuli replaced with novel objects (a 7 cm gray toy mouse and a 6 cm white plastic cup; use of either as the lone novel object in phase 1 randomized across mice) approximating in size as a mouse. Behavior was measured and data analyzed as for social approach.

Anxiety- and stress-related phenotypes, corticolimbic dendritic spine density and morphology and forebrain microarray analysis

Light/dark exploration test

The light/dark exploration test (7, 25) consisted of 2 compartments (each 17 x 13 x 13 cm), 1 with white Plexiglas walls and clear Plexiglas floor (40 lux) ('light' compartment) and the other with black Plexiglas walls and clear Plexiglas floor (0 lux) ('dark' compartment) that were connected by a partition at floor level with a small opening (5 cm) (Med Associates, Georgia, VT, Model ENV-3013). The mouse was placed into the dark compartment facing away from the aperture and allowed to explore the apparatus for 10 min. Time spent and full-body transitions into the light compartment, and total full-body transitions between the compartments was measured by photocells connected to Med Associates software. Genotypes were compared using unpaired *t*-tests.

Elevated plus-maze

The elevated plus-maze (26, 27) consisted of 2 open arms (30 x 5 cm; 90 lux) and 2 closed arms (30 x 5 x 15 cm; 20 lux) extending from a 5 x 5 cm central area and elevated 20 cm from the ground (San Diego Instruments, San Diego, CA). The walls were made from black ABS plastic and the floor from white ABS plastic. A 0.5 cm raised lip around the perimeter of the open arms prevented mice from falling off the maze. Testing was conducted under 65 dB white noise to minimize external noise disturbances (Sound Screen, Marpac Corporation, Rocky Point, NC). The mouse was placed facing an open arm in one experiment, and facing a closed arm in another experiment (separate cohort of mice) and allowed to explore the apparatus for 5 min.

Time spent in the open arms and open and closed arm entries was measured by the Ethovision videotracking system. Genotypes were compared using unpaired *t*-tests.

Stress-induced hyperthermia

Stress-induced hyperthermia (28) was assessed by taking 2 core body temperature, 10 min apart, via insertion of a Thermalert TH-5 thermometer (Physitemp, Clifton, NJ, USA) 2 cm into the rectum until a stable reading was given. The difference between the 2 readings (delta temperature) was taken as the dependent variable. Genotypes were compared using unpaired *t*-test.

Stress-induced serum corticosterone

Serum corticosterone was assessed following exposure to 30 min of restraint in 50 mL Falcon tubes, as previously described (29). The mouse was then immediately sacrificed via rapid cervical dislocation and trunk blood collected after decapitation. Non-stressed controls were sacrificed immediately after removal from the home cage. Blood samples were centrifuged at 13,000 rpm for 30 sec. Serum was extracted and assayed for total corticosterone (bound and free) analyzed using the ImmuChem Double Antibody RIA kit (limit of detection: 7.7 ng/ml; MP Biomedicals, Orangeburg NY) as previously described (30). Genotype x stress effects were analyzed using 2-factor ANOVA, followed by Fisher's LSD *post hoc* tests.

Corticolimbic dendritic spine density and morphology

The density and morphology of dendritic spines on neurons in two key corticolimbic regions mediating anxiety and stress, basolateral amygdala (BLA) and anterior cingulate cortex

(ACC), were measured via biolistic labeling as previously described (12). Coronal brain slices (200 μm) were cut on a vibratome (Leica VT 1200S, Bannockburn, IL) and fixed in 4% paraformaldehyde/4% sucrose solution for 30 min at room temperature, then washed several times with PBS. Particle-mediated ballistic delivery of fluorescent dyes was performed based on methods previously described (31, 32) Briefly, neurons were labeled by shooting the slices with tungsten beads (1.7 μm in diameter, BioRad, Hercules, CA) coated with DiI (1-1'-dioctadecyl-3,3,3',3'-tetramethyl-indocarbocyanine perchlorate) (Invitrogen, Carlsbad, CA) using a biolistic Helios gene gun (BioRad) (180 psi helium gas pressure) through a membrane filter with a 3 μm pore size (Falcon 3092; BD Biosciences, Franklin Lakes, NJ). Slices were rinsed with PBS and mounted on slides using ProLong Antifade Gold (Invitrogen). A confocal microscope (Zeiss LSM 5, Pascal, Thornwood, NY) was used to acquire a stack of images (z-spacing= 0.8 μm) of the apical dendrites from isolated neurons in BLA and ACC using a 63X oil objective (N.A=1.4) at 1.2 μm optical section. Regions with overly dense clusters of DiI stained cells were avoided. Three to five dendrites per cell were imaged (215 x 215 pixels, x-y scaling=0.0952 μm/pixel) and at least 3 cells per mouse collected. All dendrites were secondary branches from the apical dendritic tree, and of a similar distance from the cell body across genotypes. Genotype effects on spine density were measured at the level of individual spines and neuron averages using Kolmogorov-Smirnov tests.

Dendritic spine morphology was analyzed using ImageViewer (33), a custom software for spine analysis written in Matlab (The MathWorks Inc, Natick, MA). Spine length was measured from the dendritic shaft junction to the spine tip. To measure spine head width, a line was drawn across the thickest part of the spine head, parallel to the dendrite, and the fluorescence distribution along this line was determined. Width was defined as width at which fluorescent

intensity fell to 30% of maximum. Spine head width was measured after categorizing spines by relative length, as follows: small=<1 μm, medium=1-2.5 μm, large=>2.5 μm. Genotype effects on spine head width and spine length was measured using the Kolmogorov-Smirnov test.

Microarray analysis, RT-PCR and Western blot

For microarray analysis, forebrain tissue was dissected and frozen in liquid nitrogen. RNA extraction was performed immediately after the final dissection using Qiagen RNeasy (Qiagen, Valencia, CA) columns according to manufacturer's protocol. Integrity and quality of the RNA was analyzed on an Agilent 2100 Bioanalyser using an Agilent RNA 6000 Nano Kit according to manufacturer's instructions. First strand cDNA synthesis from the RNA samples was performed with a SuperScript II kit (Invitrogen, Carlsbad, CA), using a GeneChip T7-dT(24) primer and 10 μg starting material. Second strand synthesis was performed using E. coli DNA polymerase (Invitrogen, Carlsbad, CA), resulting in a double stranded cDNA product that was cleaned with a phenol-chloroform extraction, followed by ethanol precipitation. An *in vitro* transcription reaction was performed on the double stranded cDNA with biotin labeled ribonucleases using T7 RNA polymerase and the Affymetrix EnzoBioArray High Yield RNA Transcription labeling kit according to manufacturer's protocol, resulting in biotin labeled cRNA which was fragmented for hybridization. cRNA was then hybridized to Affymetrix U74av2 arrays according to the manufacturer's instructions. Following hybridization, the arrays were stained with streptavidin-phycoerythirin and arrays were scanned with the Affymetrix GeneChip Scanner 2500. Analysis was performed using the Affymetrix MAS 5.1 software in accordance with manufacturer's protocols. Significant alterations were observed in: *Atp7a* (ATPase, Cu++ transporting, alpha polypeptide), *Sptlc2* (serine palmitoyltransferase long chain base subunit 2),

Sdcbp (syndecan binding protein, aka syntenin-1), *Nr4a1* (nuclear receptor subfamily 4 aka nur77), *Fos* (cfos), *Egr2* (early growth response 2), *Per1* (period homolog 1), *Junb* (JunB), *Cyln2* (cytoplasmic linker protein of 115 kDa, aka CLIP-115), *Gadd45b* (growth arrest and DNA-damage-inducible 45 beta), RIKEN cDNA 5730408C10, cDNA sequence BC005632, and RIKEN cDNA 1110007M04.

Changes in a subset of genes that were 1) significantly different between genotypes and 2) exceeded a fold-difference threshold of 1.5 were confirmed by quantitative RT-PCR. For RT-PCR, strand cDNA was made from 0.5 μg RNA, using oligo dT primers, with RETROscript (Ambion, Austin, TX). RNA was made up to 10 μl with dH_2O and incubated with 2 μl oligo dT for 3 min at 70°C. 4 μl 10 mM dNTPs, 2 μl buffer, 1 μl RNase Inhibitor and 1 μl m-MLV reverse transcriptase was added and samples incubated for 1 hr at 42°C. The enzyme was then heat inactivated at 92°C for 10 min. PCR was carried out using the DNA Engine Opticon LightCycler (MJ Research). Reactions were set up as follows. For sample wells 2 μl cDNA, 2.5 μl primers (forward and reverse primers at 2.5μM) and 8 μl H_2O were mixed with 12.5 μl 2x Quantitect SYBR Green PCR Master Mix (Qiagen, Valencia, CA), containing SYBR green dye, dNTPs and HotStarTaq DNA Polymerase. Wells for the standard curve for each primer pair were set up using 2 μl of 1, 2, 4 and 8 fold dilutions of a standard cDNA from *Dlg4*$^{+/+}$ forebrain RNA. These dilutions were attributed the values of 2000, 1000, 500 and 250 units to represent the amount of cDNA in the samples. All reaction conditions were as follows: 95°C for 15s, (94°C for 15 sec, 55°C for 30 sec, 72°C for 30 sec) x 35, then melting curve run from 60°C to 90°C with a read every 1°C; with a hold for 1 sec between reads. The melting curves were examined to ensure each primer pair had only one double stranded product. mRNA levels were

calculated from triplicate values from 3 *Dlg4*$^{+/+}$ and 3 *Dlg4*$^{-/-}$ mice, normalized to GAPDH levels and compared across genotype using unpaired *t*-tests (Table S2).

Western blot analysis was conducted to confirm *Cyln2* downregulation at the protein level. Forebrain tissue was homogenized in 50 mM Tris-HCl, 1% sodium deoxycholate, 50 mM NaF, 20 mM $ZnCl_2$, 1 mM sodium orthovanadate, 0.5 mg/ml PMSF, and Protease Inhibitors Complete (Roche Molecular Biochemicals, Indianapolis, IN). Proteins were separated by SDS-PAGE (25 μg per lane). Standard procedures were used for western blotting; samples were separated by SDS-PAGE and transferred to PVDF membrane at 4°C for 90 min at 75 V in 10% (v/v) methanol and 10 mM CAPS, pH 11.0. Primary antibody for Cyln2 (ab58057, Abcam, Cambridge, MA) was used at 1 $\mu g ml^{-1}$. Signals were detected using peroxidase-linked secondary IgGs and enhanced chemiluminescence. Data were normalized to β-tubulin and genotype differences were compared using unpaired *t*-test.

Locomotor function, motor coordination and cerebellar morphology

Novel open field exploration

The novel open field test was conducted as previously described (34). The mouse was placed in the perimeter of a 39 x 39 x 35 cm square arena constructed of white Plexiglas and allowed to explore the apparatus for 60 min. Testing was conducted under 65 dB white noise to minimize external noise disturbances (Sound Screen, Marpac Corporation, Rocky Point, NC). Total distance traveled in the whole arena and whole-session time spent in the central 20 x 20 cm was measured by the Ethovision videotracking system (Noldus Information Technology Inc., Leesburg, VA). Genotype x time effects were analyzed using 2-factor ANOVA, with repeated measures for time. Genotypes were compared for percent center time using unpaired *t*-test.

Effects of MPEP on novel open field exploration

A 10-min novel open field test was repeated (in a new cohort) as above 30 min after i.p. injection of 10 mg/kg MPEP or saline vehicle. Genotype x drug effects on total distance traveled were analyzed using 2-way ANOVA.

Home cage activity

Home cage activity was assessed as previously described (34). The mouse was first placed in a standard home cage under normal *vivarium* conditions and left undisturbed for a 48 hr acclimation period. Activity was then measured during the light and dark phases over 24 hr using the photocell-based Opto M3 activity monitor (Columbus Instruments, Columbus, OH). Genotype x light/dark cycle effects were analyzed using 2-factor ANOVA, with repeated measures for cycle.

Accelerating rotarod

Motor coordination was assessed using the accelerating rotarod as previously described (35). The apparatus was a Med Associates rotarod (model ENV-577) with a 7-cm-diameter dowel covered with 320 grit sandpaper to provide a uniform surface that prevented mice gripping the rubberized dowel. The mouse was placed onto the rotarod dowel which was then accelerated at a constant rate of 8 rpm/min up to 40 rpm. The latency to fall to the floor 10.5 cm below was automatically recorded by photocell beams, with a maximum cutoff latency of 5 min. There were 10 training trials separated by a 30-sec inter-trial interval. Genotype x trial effects were analyzed using 2-factor ANOVA, with repeated measures for trial.

Balance beam

The balance beam test was conducted as previously described (35). The mouse was placed at one end of a 40-cm long smooth, machined texture beam traversing a 40-cm-high drop. The time taken to cross from one side of the beam to the other and the number of foot slips was measured. If the mouse did not spontaneously walk to the other end, lightly pinching the tail or haunches prompted walking. The mouse was tested on 3 beams of decreasing width (1.5, 1.0, 0.75 cm), with 4 trials (30-sec inter-trial interval) on each beam (20 min inter-beam interval) and scores averaged for each beam. Genotype x beam-width effects on average foot slips were analyzed using 2-factor ANOVA, with repeated measures for beam-width.

Inverted wire-hang

The inverted wire-hang test was applied as previously described (35). The mouse was placed on a grid surface made of 2-mm diameter metal rods running lengthwise at 10-mm intervals. The grid surface was slowly rotated until the mouse was hanging upside down. Genotypes were compared for latency to fall using unpaired *t*-test.

Cerebellar morphology

Brains were fixed in 4% formaldehyde in PBS and 50 μm vibratome sections taken in the sagittal plane through the cerebellar vermis. Sections were incubated for 1 hr in PBS-T (Phosphate-Buffered Saline, 0.2% Triton X-100, pH 7.4), blocked for 2 hr with 5% bovine serum albumin in PBS-T followed by an overnight incubation at 4^{o}C with rabbit anti-calbindin (1:500, Swant, Bellinzona, Switzerland) and chicken anti-neurofilament (1:1000, Encor Biotechnology,

Gainesville, FL) diluted in PBS-T. Sections were washed 3 times for 30 min in PBS-T then incubated in Alexa 568 goat anti-rabbit antibody (1:1000, Invitrogen, Carlsbad, CA) and Alexa 488 goat anti-chicken (1:1000, Invitrogen, Carlsbad, CA) overnight at 4^{o}C. Control sections were prepared by omission of the primary antibody. Sections were washed again 3 times for 30 min then incubated for 20 min in 4′,6-diamidino-2-phenylindole (D3571, Invitrogen, Carlsbad, CA) diluted to 0.5 μg/mL in PBS-T. Sections were washed twice for 5 min then mounted from Tris-buffered saline (25 mM Tris, 145 mM NaCl, pH 7.4) and allowed to partially dry onto Superforst Plus^{TM} slides. Slides were cover slipped in 3M (PBS, 50% glycerol, saturated with n-propyl gallate). Slides were sealed with nail polish and stored in a humidified environment at 4^{o}C. All incubations were performed on a rocking platform in a light-free environment.

Sections were imaged in fluorescence with a Zeiss Axioplan 2 Imaging microscope using a 10x, NA .32 Plan-Apochromat objective. DAPI was imaged using 350/50 nm excitation and 460/50 nm emission filters. Alexa 488 was imaged using 480/40 nm excitation and 535/30 nm emission filters and Alexa 568 was imaged using 535/50 nm excitation and 610/75 nm emission filters. Images were captured and subsequently pseudo-colored using a Hamamatsu Orca CCD monochrome camera and Ivision by Biovision software. Several focal planes were captured and processed together, and the 3 channels (red, green and blue) superimposed using Adobe Photoshop software.

Structural MRI of mouse brain

MRI analysis was performed on a horizontal bore 7 Tesla scanner operating on a Bruker Avance platform (Bruker Biospin Inc. Bellerica, MA). Mice were perfused with saline, brains extracted and placed in 10% formalin. Prior to MRI, the brain was removed from formalin and

the surface moisture on the brain removed. The brain was then placed in a 12 mm NMR tube (Wilmad lab glass, Buena, NJ) and submerged in fluorinated liquid, Fomblin (Ausimont, NJ, USA) to minimize any image artifacts resulting from magnetic susceptibility differences between the tissue and surrounding air, and to eliminate any intense water signal affecting tissue contrast. The brain was centered in a 13 mm, 3 turn solenoid radio frequency coil. A scout image producing 3 mutually perpendicular images through the excised brain was acquired using a Gradient echo sequence (Repetition Time [TR]/Echo Time [TE]=100/6 ms, 30° flip angle, in-plane resolution=200 μm, slice thickness=1 mm). These images were used to obtain the optimum volumetric field of view that encompasses the whole brain for the subsequent 3-D scan. A fast spin echo image sequence, with a TR/TE=2600/12.5 ms and echo train length [RARE factor]=4, 2 averages, and 3-D Field of view=19.2 mm, was used to achieve an isotropic resolution of 67 μm in a total scan time of 13.25 hours. Genotypes were compared for total brain volume using unpaired *t*-tests.

Human genotyping and neuroimaging

Subjects were recruited as part of an ongoing multi-center study examining the influence of genetic variation on intermediate neuroimaging phenotypes related to neuropsychiatric conditions, as described previously (36). Sixty-two participants were recruited from Mannheim and 51 from Bonn (Table S3). All participants were German and had parents and grandparents from European origin. No participant had lifetime or family history of a major psychiatric disorder. All subjects completed an imaging genetics protocol that included several functional magnetic imaging (fMRI) measurements, and structural MRI voxel based morphometry (37). The final fMRI analysis comprised data from 115 subjects, and the structural MRI 93 subjects.

Subjects gave written informed consent and the local ethics committees of Heidelberg and Bonn Universities approved the study.

Subjects underwent genome-wide Single Nucleotide Polymorphism (SNP) analysis. Genomic DNA was prepared from whole blood according to standard procedures. SNP genotypes were assigned using the Illumina Human610-quad beadchip (Illumina Inc., San Diego, CA). The following quality assurance criteria were used: per person – callrate > 0.98, gender-check (x-chromosomal inferred sex vs. 'pedfile-sex'), IBS <1.65 to exclude cryptical relatedness, outlier analysis using EIGENSTRAT and heterozygosity per individual. No person was excluded based on these criteria. We included SNPs with a callrate >0.98, MAF >0.01 and pHWE >0.0001. Of initially 592,532 SNPs, 553,176 SNPs remained after applying these criteria, largely because of the minor allele frequency criterion (excluding n >34000).

No functional variants associated with clinical or biological phenotypes have been described in DLG4. Therefore, we based SNP selection on available coverage in the Illumina chip. In the *DLG4* gene, 4 SNPs were available on the Illumina chip of which 3 (rs17203281, rs3826408, rs390200) met quality control criteria (see below). Since linkage disequilibrium between rs17203281 and rs3826408 was high (r=0.8) we only included rs17203281 and rs390200 in our analysis. For both SNPs, genotype distributions were in Hardy Weinberg Equilibrium in our sample (rs17203281: χ^2 =0.126, df=1, *ns* rs390200: χ^2=0.021, df=1, *ns*). Since the number of homozygote A-allele carriers for rs17203281 was small (N=15), we combined AA and AG allele carriers for comparison with G allele homozygotes. The distribution of genotypes did not differ between the Bonn and Manheim collection sites. Genotype groups did not differ in terms of age, education, gender, handedness, or performance in the functional imaging task (as anayzed using Chi-squared, ANOVA and *t*-test). For details, see Table S2.

fMRI measurements were performed on 2 Trio 3T scanners (Siemens Medical Systems, Erlangen, Germany) at the Central Institute of Mental Health Mannheim and the University of Bonn. Identical sequences and scanner protocols were used at both sites. For structural imaging, 3 separate T1 weighted MPRage sequences were acquired from each subject (parameters: 160 slices of 1 mm, FOV 256 mm, resolution 256 x 256, TR 1570 ms, TE 3.42 msec). For BOLD fMRI imaging, 134 volumes were sampled during task completion (parameters: 28 slices of 4 mm, 1 mm gap, FOV 192 mm, resolution 64 x 64, TR 2 sec, TE 30, flip angle 90°). To account for saturation effects, the first 4 volumes were excluded from the analysis. Quality assurance (QA) measures were conducted on every measurement day at both sites according to a multicenter QA protocol (38) revealing stable signals over time. To stringently account for any differences in signal-to-noise across sites, site was included as a covariate for all statistical analyses.

During fMRI scanning, subjects completed the face-matching task (FMT). The FMT is a simple perceptual task that robustly engages the amygdala (39) and elicits altered amygdala activation and connectivity with cortical regions in WBS subjects (40). Subjects indicated which 2 of 3 simultaneously presented emotional faces (anger, fear) were the same. Emotion blocks alternated with 4 blocks of a sensorimotor control task where faces were replaced with simple geometric shapes. Both conditions were presented 4 times each with a block length of 30 sec. Instruction was given between blocks for 2 sec, resulting in a total task time of around 4 min 30 sec. Processing and statistical analyses of the fMRI data were conducted using statistical parametric mapping methods as implemented in SPM5 (The Wellcome Trust Center for Neuroimaging, http://www.fil.ion.ucl.ac.uk/spm/software/spm5). First, images were realigned to a mean image and then slice time corrected, spatially normalized to a standard stereotactic space

[a brain template created by the Montreal Neurological Institute (MNI)] with volume units (voxels) of 3 x 3 x 3 mm and smoothed with an 9 mm FWHM (full width at half maximum) Gaussian filter. Statistical contrast images of the emotion task versus sensorimotor control were then obtained for each subject.

Regions of interest (ROI) were defined in the amygdala and subgenual anterior cingulate cortex (sgACC) based upon abnormal recruitment of these regions during the FMT in WBS subjects (40). The amygdala mask used for seed voxel extraction and ROI analyses was created using anatomical labels provided by the Wake Forest University PickAtlas (www.fmri.wfubmc.edu/downloads), and the sgACC mask was created using the MARINA software (41). To analyze amygdala-sgACC connectivity, a seed region approach was employed as recently described (36). For each subject, the first eigenvariates from all voxels within an anatomical amygdala mask were calculated. To derive a robust summary measure of activity in the amygdala ROI, we excluded white-matter by restricting the averaging to voxels related to task at a $p<.05$ level; NB, this threshold was not used for statistical inference but to exclude non gray matter voxels. Using SPM5, seed timeseries were temporally filtered and task related variance was removed. To account for noise, the first eigenvariates from masks covering cerebrospinal fluid (CSF) and white matter were extracted for each individual and each task and entered, together with movement covariates, into whole brain multiple regression first level analyses, where seed region activity was the covariate of interest. The resulting maps of partial correlation of timeseries of BOLD signal measurements in all voxels, with the BOLD timeseries in the seed region, were then subjected to a random effects analysis in SPM5 as described above. Genotype effects on neural activation and cortico-amygdala connectivity were analyzed using the general linear model in a second-level random effects analysis, with genotype as covariate of

interest and scanner site as a nuisance covariate. Significant regression data were followed up with Bonferroni corrected Fisher's LSD *post hoc* comparison between genotypes. For all imaging methods, significance threshold was $p<.05$, corrected for multiple comparisons within regions of interest. We used family-wise error (FWE), based on Gaussian Random Fields theory, and false discovery rate (FDR), a widely used frequentist method, both of which strongly control for type I error in imaging genetics (42).

For the voxel based morphometry (VBM) analysis, The 3 T1 volumes were first realigned using the motion correction algorithm as implemented in SMP5. The mean image of this realignment step was then used for further analysis using the VBM5 toolbox (http://dbm.neuro.uni-jena.de/vbm). Briefly, the images were first bias- corrected, then segmented into gray and weight matter as well as CSF and then normalized using different tissue probability maps. The resulting gray matter images were smoothed using a 12 mm (FWHM) Gaussian filter. For statistical analysis the modulated images representing gray matter density were included into a second level random effect analysis with genotype as the covariate of interest, and age, sex, total brain volume and site as nuisance variables. ROI was defined for the occipital/intraparietal cortex based upon evidence of reduced gray matter volume in WBS patients (43). ROIs were defined as 20 mm spheres around the most significant voxel. Genotypes were compared using unpaired *t*-tests.

REFERENCES

1. Yao WD, Gainetdinov RR, Arbuckle MI, Sotnikova TD, Cyr M, Beaulieu JM, Torres GE, Grant SG, Caron MG: Identification of PSD-95 as a regulator of dopamine-mediated synaptic and behavioral plasticity. Neuron 2004; 41(4):625-38
2. Arbuckle MI, Komiyama NH, Forsyth LH, Bence M, Ainge JA, Feyder M, Holmes A, Wood ER, Carlisle HJ, O'Dell TJ, Grant SGN: Phenotype in Post Synaptic Density 95 null mutant mice recapitulates PSD-95 mutant mice. submitted
3. Millstein RA, Holmes A: Effects of repeated maternal separation on anxiety- and depression-related phenotypes in different mouse strains. Neurosci Biobehav Rev 2007; 31(1):3-17
4. Migaud M, Charlesworth P, Dempster M, Webster LC, Watabe AM, Makhinson M, He Y, Ramsay MF, Morris RG, Morrison JH, O'Dell TJ, Grant SG: Enhanced long-term potentiation and impaired learning in mice with mutant postsynaptic density-95 protein. Nature 1998; 396(6710):433-9
5. McIlwain KL, Merriweather MY, Yuva-Paylor LA, Paylor R: The use of behavioral test batteries: effects of training history. Physiol Behav 2001; 73(5):705-17
6. Crawley JN, Paylor R: A proposed test battery and constellations of specific behavioral paradigms to investigate the behavioral phenotypes of transgenic and knockout mice. Horm Behav 1997; 31(3):197-211
7. Boyce-Rustay JM, Holmes A: Genetic inactivation of the NMDA receptor NR2A subunit has anxiolytic- and antidepressant-like effects in mice. Neuropsychopharmacology 2006; 31(11):2405-14
8. Millstein RA, Ralph RJ, Yang RJ, Holmes A: Effects of repeated maternal separation on prepulse inhibition of startle across inbred mouse strains. Genes Brain Behav 2006; 5(4):346-54
9. Geyer MA, McIlwain KL, Paylor R: Mouse genetic models for prepulse inhibition: an early review. Mol Psychiatry 2002; 7(10):1039-53
10. Wrenn CC, Harris AP, Saavedra MC, Crawley JN: Social transmission of food preference in mice: methodology and application to galanin-overexpressing transgenic mice. Behav Neurosci 2003; 117(1):21-31

11. Bannerman DM, Niewoehner B, Lyon L, Romberg C, Schmitt WB, Taylor A, Sanderson DJ, Cottam J, Sprengel R, Seeburg PH, Kohr G, Rawlins JN: NMDA Receptor Subunit NR2A Is Required for Rapidly Acquired Spatial Working Memory But Not Incremental Spatial Reference Memory. J Neurosci 2008; 28(14):3623-30
12. Brigman J, Lovinger DM, Holmes A: GluN2B and memory. J Neurosci 2010
13. Blundell J, Blaiss CA, Etherton MR, Espinosa F, Tabuchi K, Walz C, Bolliger MF, Sudhof TC, Powell CM: Neuroligin-1 deletion results in impaired spatial memory and increased repetitive behavior. J Neurosci 2010; 30(6):2115-29
14. Silverman JL, Tolu SS, Barkan CL, Crawley JN: Repetitive self-grooming behavior in the BTBR mouse model of autism is blocked by the mGluR5 antagonist MPEP. Neuropsychopharmacology 2010; 35(4):976-89
15. Zhao S, Edwards J, Carroll J, Wiedholz L, Millstein RA, Jaing C, Murphy DL, Lanthorn TH, Holmes A: Insertion mutation at the C-terminus of the serotonin transporter disrupts brain serotonin function and emotion-related behaviors in mice. Neuroscience 2006; 140(1):321-34
16. Scattoni ML, Gandhy SU, Ricceri L, Crawley JN: Unusual repertoire of vocalizations in the BTBR T+tf/J mouse model of autism. PLoS One 2008; 3(8):e3067
17. Champlin AK: Suppression of oestrus in grouped mice: the effects of various densities and the possible nature of the stimulus. J Reprod Fertil 1971; 27(2):233-41
18. Jamain S, Radyushkin K, Hammerschmidt K, Granon S, Boretius S, Varoqueaux F, Ramanantsoa N, Gallego J, Ronnenberg A, Winter D, Frahm J, Fischer J, Bourgeron T, Ehrenreich H, Brose N: Reduced social interaction and ultrasonic communication in a mouse model of monogenic heritable autism. Proc Natl Acad Sci U S A 2008; 105(5):1710-5
19. Champlin AK, Dorr DL, Gates AH: Determining the stage of the estrous cycle in the mouse by the appearance of the vagina. Biol Reprod 1973; 8(4):491-4
20. Wiedholz LM, Owens WA, Horton RE, Feyder M, Karlsson RM, Hefner K, Sprengel R, Celikel T, Daws LC, Holmes A: Mice lacking the AMPA GluR1 receptor exhibit striatal hyperdopaminergia and 'schizophrenia-related' behaviors. Mol Psychiatry 2008; 13(6):631-40
21. Moy SS, Nadler JJ, Perez A, Barbaro RP, Johns JM, Magnuson TR, Piven J, Crawley JN: Sociability and preference for social novelty in five inbred strains: an approach to assess autistic-like behavior in mice. Genes Brain Behav 2004; 3(5):287-302

22. Brigman JL, Ihne J, Saksida LM, Bussey TJ, Holmes A: Effects of Subchronic Phencyclidine (PCP) Treatment on Social Behaviors, and Operant Discrimination and Reversal Learning in C57BL/6J Mice. Front Behav Neurosci 2009; 3:2
23. Nadler JJ, Moy SS, Dold G, Trang D, Simmons N, Perez A, Young NB, Barbaro RP, Piven J, Magnuson TR, Crawley JN: Automated apparatus for quantitation of social approach behaviors in mice. Genes Brain Behav 2004; 3(5):303-14
24. Bear MF, Dolen G, Osterweil E, Nagarajan N: Fragile X: translation in action. Neuropsychopharmacology 2008; 33(1):84-7
25. Crawley JN: Neuropharmacologic specificity of a simple animal model for the behavioral actions of benzodiazepines. Pharmacol Biochem Behav 1981; 15(5):695-9
26. Handley SL, Mithani S: Effects of alpha-adrenoceptor agonists and antagonists in a maze-exploration model of 'fear'-motivated behaviour. Naunyn Schmiedebergs Arch Pharmacol 1984; 327(1):1-5
27. Yang RJ, Mozhui K, Karlsson RM, Cameron HA, Williams RW, Holmes A: Variation in Mouse Basolateral Amygdala Volume is Associated With Differences in Stress Reactivity and Fear Learning. Neuropsychopharmacology 2008
28. Lecci A, Borsini F, Volterra G, Meli A: Pharmacological validation of a novel animal model of anticipatory anxiety in mice. Psychopharmacology (Berl) 1990; 101(2):255-61
29. Mozhui K, Karlsson RM, Kash T, Ihne J, Norcross M, Patel S, Farrell MR, Hill EE, Martin KP, Camp M, Fitzgerald P, Ciobanu DC, Sprengel R, Mishina M, Wellman CL, Winder D, Williams RW, Holmes A: Strain differences in stress responsivity are associated with divergent amygdala gene expression and glutamate-mediated neuronal excitability. J Neurosci 2010; in press
30. Boyce-Rustay JM, Cameron HA, Holmes A: Chronic swim stress alters sensitivity to acute behavioral effects of ethanol in mice. Physiol Behav 2007; 91(1):77-86
31. Grutzendler J, Tsai J, Gan WB: Rapid labeling of neuronal populations by ballistic delivery of fluorescent dyes. Methods 2003; 30(1):79-85
32. Lee KW, Kim Y, Kim AM, Helmin K, Nairn AC, Greengard P: Cocaine-induced dendritic spine formation in D1 and D2 dopamine receptor-containing medium spiny neurons in nucleus accumbens. Proc Natl Acad Sci U S A 2006; 103(9):3399-404

33. Steiner P, Higley MJ, Xu W, Czervionke BL, Malenka RC, Sabatini BL: Destabilization of the postsynaptic density by PSD-95 serine 73 phosphorylation inhibits spine growth and synaptic plasticity. Neuron 2008; 60(5):788-802

34. Karlsson RM, Heilig M, Holmes A: Loss of glutamate transporter GLAST (EAAT1) causes locomotor hyperactivity and exaggerated responses to psychotomimetics: rescue by haloperidol and mGlu2/3 agonist. Biol Psychiatry 2008; in press

35. Boyce-Rustay JM, Holmes A: Functional roles of NMDA receptor NR2A and NR2B subunits in the acute intoxicating effects of ethanol in mice. Synapse 2005; 56(4):222-5

36. Esslinger C, Walter H, Kirsch P, Erk S, Schnell K, Arnold C, Haddad L, Mier D, Opitz von Boberfeld C, Raab K, Witt SH, Rietschel M, Cichon S, Meyer-Lindenberg A: Neural mechanisms of a genome-wide supported psychosis variant. Science 2009; 324(5927):605

37. Friston KJ, Penny W, Phillips C, Kiebel S, Hinton G, Ashburner J: Classical and Bayesian inference in neuroimaging: theory. Neuroimage 2002; 16(2):465-83

38. Friedman L, Glover GH: Report on a multicenter fMRI quality assurance protocol. J Magn Reson Imaging 2006; 23(6):827-39

39. Hariri AR, Tessitore A, Mattay VS, Fera F, Weinberger DR: The amygdala response to emotional stimuli: a comparison of faces and scenes. Neuroimage 2002; 17(1):317-23

40. Meyer-Lindenberg A, Hariri AR, Munoz KE, Mervis CB, Mattay VS, Morris CA, Berman KF: Neural correlates of genetically abnormal social cognition in Williams syndrome. Nat Neurosci 2005; 8(8):991-3

41. Walter B, Blecker C, Kirsch P, Sammer G, Schienle A, Stark R, Vaitl D: MARINA: An easy to use tool for the creation of MAsks for Region of INterest Analyses Neuroimage 2003; 19(S2):Supplement (CD)

42. Meyer-Lindenberg A, Nicodemus KK, Egan MF, Callicott JH, Mattay V, Weinberger DR: False positives in imaging genetics. Neuroimage 2008; 40(2):655-61

43. Meyer-Lindenberg A, Kohn P, Mervis CB, Kippenhan JS, Olsen RK, Morris CA, Berman KF: Neural basis of genetically determined visuospatial construction deficit in Williams syndrome. Neuron 2004; 43(5):623-31

Table S1: Basic screen. Genotypes did not differ significantly on any measure. Data are the percentage of each genotype showing the measure, unless a unit of measurement is shown (in which case data are Means ±SEM). n=13-22/genotype.

	Dlg4$^{+/+}$	*Dlg4*$^{-/-}$
Physical health		
Bald patches	0	0
Body weight (g)	22.2 ± .9	20.5 ± .8
Core body temperature (ºC)	38.5 ± .1	38.4 ± .1
Exophthalmus	0	0
Kinked tail	0	0
Kyphosis	0	0
Lordosis	0	0
Missing whiskers	0	10
Piloerection	0	0
Straub tail	0	0
Sensory reflexes		
Approach response	100	100
Palpebral response	100	100
Pinna reflex	100	100
Tail pinch response	100	100
Touch response	100	100
Motor, neurological		
Forepaw clutch	0	0
Hindpaw clutch	0	0
Splayed limbs	0	0
Empty cage behaviors		
Abnormal gait	0	0
Circling	0	0

Defecation	27	23
Freezing	0	8
Grooming	55	31
Head bobbing	0	0
Licking	0	0
Jumping	0	0
Prancing forelimbs	0	0
Rearing	95	62
Retropulsion	0	0
Seizure	0	0
Sniffing	100	92
Trembling	5	8
Urination	0	0
Wild running	0	0

Table S2: Confirmation of microarray results by quantitative RT-PCR in wild type and *Dlg4*$^{-/-}$ forebrain. Table shows the average levels of *Fos*, *Egr2*, *Nr4a1*, *Sdcbp* and *MAP2B* in wildtype and *Dlg4*$^{-/-}$ forebrain (calculated from triplicate values from 3 wild type and 3 mutant samples, normalised by GAPDH levels). The fold change and *P* value calculated by a Student's *t*-test for each gene is shown.

	Ave. *Dlg4*$^{+/+}$	Ave. *Dlg4*$^{-/-}$	Fold Change	*p* value
Down Regulated				
Fos	2.06	0.282	7.30	0.033
Egr2	0.090	0.022	4.09	0.047
Nr4a1	0.022	0.0068	3.24	0.046
Up Regulated				
Sdcbp	0.0005	0.0019	3.80	0.047
No Change				
MAP2B	0.655	0.557	1.18	0.67

Table S3: Details of human subjects. Distribution of demographic and fMRI performance did not differ between genotypes. Data are number of subjects or Means ±SD.

	rs17203281 genotype	
	AA/AG	GG
N (Bonn/Mannheim)	60 (28/32)	53 (23/30)
Male/female	25/35	24/29
Left handed	4	5
Age (years)	33.5 (10.5)	33.1 (9.8)
School education (years)	11.9 (1.5)	11.9 (1.6)
Percent correct answers during face matching	97.9 (4.9)	98.5 (3.6)
Reaction times: face matching minus form matching (msec)	167.5 (159.9)	119.5 (167.2)

	rs390200 genotype		
	AA	AG	GG
N (Bonn/Mannheim)	20 (6/14)	52 (26/26)	41 (19/22)
Male/female	9/11	19/33	21/20
Left handed	1	5	3
Age (years)	35.6 (10.3)	33.2 (10.6)	32.5 (9.5)
School education (years)	11.8 (1.5)	12.0 (1.6)	11.9 (1.6)
Percent correct answers during face matching	98.8 (3.1)	97.4 (4.8)	98.9 (4.2)
Reaction times: face matching minus form matching (msec)	132.3 (184.5)	143.6 (162.1)	152.9 (160.9)

Supplemental Figures

Figure S1: Acoustic startle, sensorimotor gating, nociception and olfaction

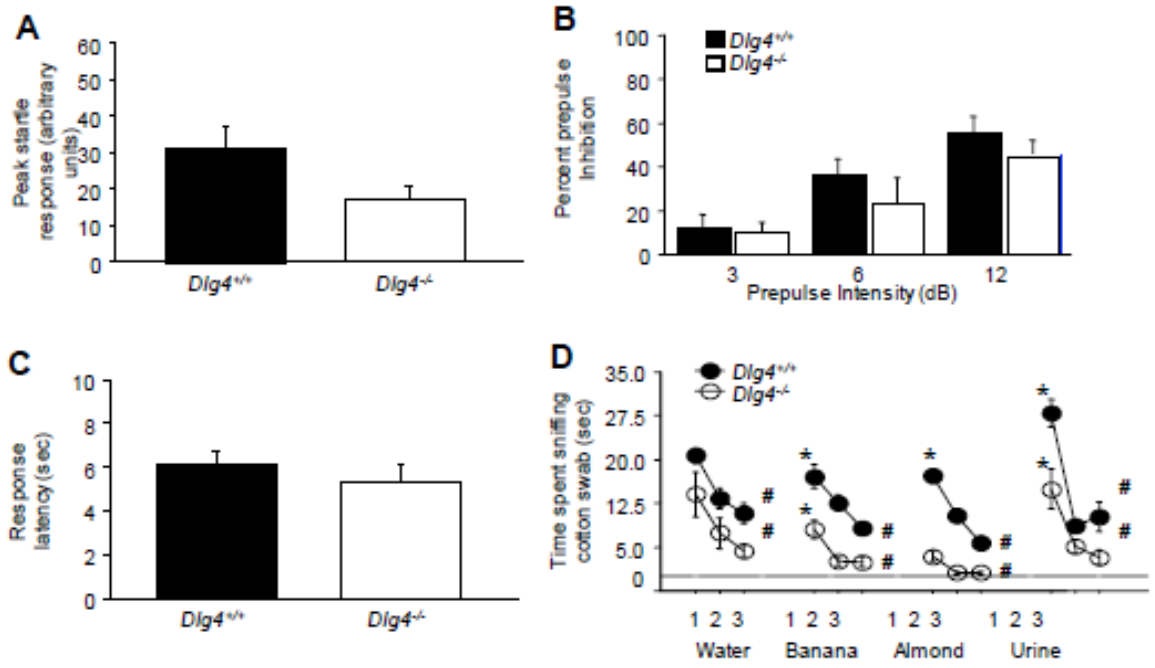

(**A**) *Dlg4*$^{-/-}$ showed a non-significant trend for a lower acoustic startle response than *Dlg4*$^{+/+}$ (n=10-19/genotype). (**B**) Genotypes did not differ in sensorimotor gating, as measured by prepulse inhibition of the acoustic startle response (n=10-19/genotype). **(C)** Genotypes did not differ in latency to show a pain response on the hot plate test (n=10-19/genotype). (**D**) Both genotypes showed significantly less sniffing (i.e., habituation) during the third presentation relative to the first presentation of the water, banana, almond, and male urine scents. Both genotypes showed significantly more sniffing (i.e., dishabituation) during the first presentation of banana and male urine scents, while *Dlg4*$^{+/+}$, but not *Dlg4*$^{-/-}$, increased investigation of the almond scent after the banana scent (n=15-19/genotype). Overall, *Dlg4*$^{-/-}$ spent less time than *Dlg4*$^{+/+}$ exploring a cotton-swab regardless of whether the swab was scented or not. Data are Means ±SEM. **p*<.05 vs. third presentation of previous scent; #*p*<.05 vs. first presentation of same scent.

Figure S2: Cortical neuronal spine density and morphology

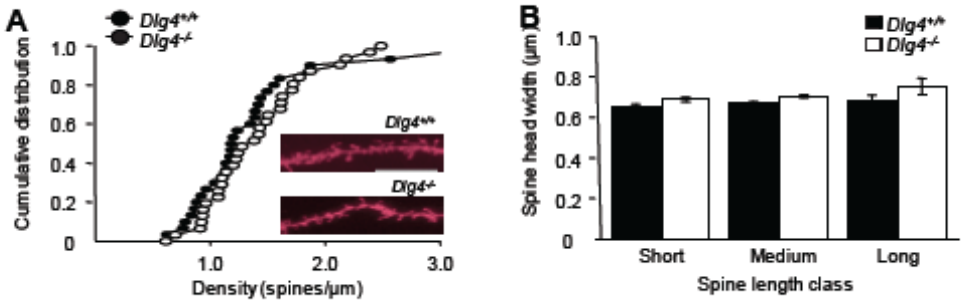

(**A,B**) *Dlg4*$^{-/-}$ showed normal headwidth of dendritic spines in anterior cingulate cortex (ACC) neurons, regardless of spine length, and normal spine density distribution (scale bar=10 µm) (n=4-5 mice per genotype, 16 neurons, 31-32 dendrites). Data are means ±SEM.